

Highlights

Physics-informed Neural Network Combined with Characteristic-Based Split for Solving Navier–Stokes Equations

Shuang Hu, Meiqin Liu, Senlin Zhang, Shanling Dong, Ronghao Zheng

- This method does not need to consider the weights between output parameters
- This method is a rapid version of Physics-informed Neural Network because not all partial derivatives participate in gradient backpropagation, and the remaining terms will be reused
- This method can solve the special form of compressible N-S equations - Shallow-Water equations, and incompressible N-S equations
- This method only needs the flow field information at a certain time to restore the past and future flow field information

Physics-informed Neural Network Combined with Characteristic-Based Split for Solving Navier–Stokes Equations[★]

Shuang Hu^{a,b}, Meiqin Liu^{c,a,*,1}, Senlin Zhang^{a,b}, Shanling Dong^{a,b} and Ronghao Zheng^{a,b}

^aCollege of Electrical Engineering, Zhejiang University, Hangzhou, 310027, China

^bState Key Laboratory of Industrial Control Technology, Zhejiang University, Hangzhou, 310027, China

^cInstitute of Artificial Intelligence and Robotics, Xi'an Jiaotong University, Xi'an, 710049, China

ARTICLE INFO

Keywords:

Physics-informed Neural Network (PINN)
Characteristic-based split (CBS) algorithm
partial differential equations (PDEs)
Navier-Stokes equations (N-S equations)

ABSTRACT

In this paper, physics-informed neural network (PINN) based on characteristic-based split (CBS) is proposed, which can be used to solve the time-dependent Navier-Stokes equations (N-S equations). In this method, The output parameters and corresponding losses are separated, so the weights between output parameters are not considered. Not all partial derivatives participate in gradient backpropagation, and the remaining terms will be reused. Therefore, compared with traditional PINN, this method is a rapid version. Here, labeled data, physical constraints and network outputs are regarded as priori information, and the residuals of the N-S equations are regarded as posteriori information. So this method can deal with both data-driven and data-free problems. As a result, it can solve the special form of compressible N-S equations—Shallow-Water equations, and incompressible N-S equations. As boundary conditions are known, this method only needs the flow field information at a certain time to restore the past and future flow field information. We solve the progress of a solitary wave onto a shelving beach and the dispersion of the hot water in the flow, which show this method's potential in the marine engineering. We also use incompressible equations with exact solutions to prove this method's correctness and universality. We find that PINN needs more strict boundary conditions to solve the N-S equation, because it has no computational boundary compared with the finite element method.

1. Introduction

The methods for solving partial differential equations (PDEs) based on neural networks are mostly data-driven. When the spatiotemporal scattered point measurement data is sufficient or the exact solution is known, using neural networks to solve CFD related parameter estimation, flow field reconstruction, proxy model construction and other problems shows great potential. Long, Lu, Ma and Dong (2018); Long, Lu and Dong (2019) proposed a feedforward neural network (PDE-Net) to invert unknown PDEs from data, in which the time derivative term is Euler discretized and the constrained convolution kernel approximates the differential operator. The method proposed in Wang, Liu and Wang (2022)'s work can reconstruct the overall velocity field and pressure field with high resolution from sparse velocity information. By adding a convection diffusion equation to N-S equations, the flow field can be restored from the concentration of the carrier in the fluid (Raissi, Yazdani and Karniadakis, 2020).

Data-driven solution has great limitations. Methods that reduce label data and rely more on known equations are widely concerned. Raissi, Perdikaris and Karniadakis

(2017a,b) proposed a physical constrained neural network (PINN). They used the control equations of PDEs and the identity of the boundary conditions to construct residuals, and used the sum of the residuals to construct the loss function. Kani and Elsheikh (2018) combined PINN with orthogonal decomposition (POD) and discrete empirical interpolation method (DEIM) to provide a high-precision reduced order model of nonlinear dynamic system, reducing the computational complexity of high fidelity numerical simulation. The adaptive swish function was proposed (Jagtap, Kawaguchi and Karniadakis, 2020), which effectively improved the efficiency, robustness and accuracy of PINN in approaching nonlinear functions and partial differential equations. Ranade, Hill and Pathak (2021) implemented a finite-volume based numerical schemes inside the computational graph, which is based on CNN. Dwivedi and Srinivasan (2020) proposed a distributed version of PINN, where the learning problem is decomposed into smaller regions of the computational domain and a physical compatibility condition is enforced in between neighboring domains. Bandai and Ghezzehei (2021) used the PINN framework composed of three DNNs to inverse the parameters of Richardson Richards equations, and achieved better results than one DNN. The multi-scale deep neural network (MscaleDNN) method was proposed to accelerate the convergence of high frequency (Wang, Zhang and Cai, 2020; Liu, Cai and Xu, 2020), the core idea is to stretch the objective function at different scales in the radial direction.

PINN has been proved to be able to solve multiple specification PDEs, and can handle multiple applications involving physics, chemistry and biology (Amini Niaki,

[★]This work was supported by the NSFC-Zhejiang Joint Fund for the Integration of Industrialization and Informatization under Grant U1809212 and the Fundamental Research Funds for the Central Universities under Grant xtr072022001.

*Corresponding author

✉ 11910077@zju.edu.cn (S. Hu); liumeiqin@zju.edu.cn (M. Liu); slzhang@zju.edu.cn (S. Zhang); shanlingdong28@zju.edu.cn (S. Dong); rzheng@zju.edu.cn (R. Zheng)

ORCID(s):

¹0000-0003-0693-6574

Haghighat, Campbell, Poursartip and Vaziri, 2021; Wang, Wang and Perdikaris, 2021; Yang, Meng and Karniadakis, 2021; Liu and Wang, 2019; Snaiki, 2019). Using PINN framework to solve more complex partial differential equations, such as N-S equations, is the focus of our work. Mao, Jagtap and Karniadakis (2020) investigated the possibility of using PINN to approximate the Euler equations that model high-speed aerodynamic flows. Mao et al. (2020) proposed Physics Informed Extreme Learning Machine (PIELM), which is a rapid version and demonstrated to solve N-S equations in a lid-driven cavity at low Reynolds numbers. Yang et al. (2021) proposed the PhysGeoNet to solve the N-S equations using the finite difference discretizations of the PDE residuals in the neural network loss formulation. Ranade et al. (2021) proposed the DiscretizationNet, which employs a generative CNN-based encoder-decoder model with PDE variables as both input and output features. DiscretizationNet is demonstrated to solve the steady, incompressible N-S equations in 3-D for several cases such as, lid-driven cavity, flow past a cylinder and conjugate heat transfer.

The core idea of this paper is to assume that the current outputs of PINN are correct, and then investigate what the future and past flow fields should be. For this reason, we introduce Characteristic-Based split (CBS) algorithm, which is widely used in the finite element method, into PINN. In the following examples, we only use the initial and boundary conditions to solve the equations without any labeled data. This method can solve the special form of compressible N-S equations—Shallow-Water equations, and incompressible N-S equations. Compared with the traditional PINN, this method does not consider the weights of output variables, and the calculation cost is smaller. We show the progress of a solitary wave onto a shelving beach and the dispersion of the hot water in the flow to explain the advantages of separating output parameters in engineering applications. By solving incompressible equations with exact solutions, we prove this method's correctness and universality.

2. PINN based on CBS

In the process of fitting data, neural networks often learn low frequencies first, and then slowly learn high frequencies. This phenomenon is called Frequency Principle (F-Principle) (Xu, Zhang and Xiao, 2019; Xu, Zhang, Luo, Xiao and Ma, 2020). Gradient descent naturally aims to eliminate low-frequency errors, while high-dimensional errors cannot be eliminated. In fact, F-Principle is also embodied in the finite element method of N-S equations, such as the limitation of time step and grid density (Codina, Vázquez and Zienkiewicz, 1998). F- principle reveals that there is high frequency disaster in the neural networks, and the training and generalization difficulties caused by high frequency disaster are difficult to be alleviated through simple parameter adjustment.

The MscaledDNN method can accelerate the convergence of high frequency. The original MscaledDNN have two similar but different network structures, shown in Fig. 1. Both network structures are better than fully connected networks. But MscaledDNN-2, which seems to have a simpler structure, shows better performance than MscaledDNN-1. Before discussing why MscaledDNN-2 is better than MscaledDNN-1, we should consider this question: is it mandatory to share parameters among output variables?

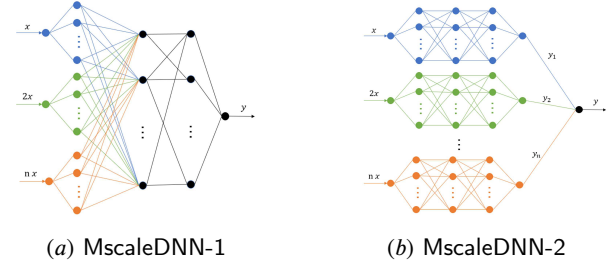


Figure 1: Two different network structures of MscaledDNN.

Suppose there is a special solution of N-S equations: the velocity u_1 in the x direction is time-varying, while the velocity u_2 in the y direction is constant, what happens when u_1 and u_2 are fully connected. u_2 is not affected by t , so the weights coefficient of t in the full connection layer will be reduced, while u_1 is time-varying and the weights reduction of t will cause the residuals about u_1 to fail to converge, and vice versa. In fact, if we observe the partial derivative of the output u_1 and u_2 to t under full connection, we will find that the two always remain at the same order of magnitude. This leads to the fact that the full connection between output parameters cannot converge in the case we mentioned above, which also explains why MscaledDNN-2 is better than MscaledDNN-1. To some extent, MscaledDNN-2 realizes the separation of output parameters.

We should have a recognition that neural networks and the finite element method belong to the time-space approximation method. The finite element method without specific algorithms can not solve complex problems, so can the neural network. After the output variables are separated, naturally we think of an algorithm commonly used in finite element method - CBS.

2.1. Characteristic-based split algorithm

The basic form of N-S equations is as follows, and the shallow-water equations and incompressible-flow equations mentioned later are its variant forms.

Conservation of mass:

$$\frac{\partial \rho}{\partial t} = \frac{1}{c^2} \frac{\partial p}{\partial t} = -\frac{\partial U_i}{\partial x_i} \quad (1)$$

Conservation of momentum:

$$\frac{\partial U_i}{\partial t} = -\frac{\partial}{\partial x_j} (u_j U_i) + \frac{\partial \tau_{ij}}{\partial x_j} - \frac{\partial p}{\partial x_i} - Q_i \quad (2)$$

where $i = \text{direction}$, $U_i = \rho u_i$, ρ is the density, p is the pressure, c is the speed of sound, u_i is the velocity component

in the i direction, and T is the absolute temperature. Q is body forces, and Q_i is the component of Q in the i direction. τ_{ij} is the deflection stress component, satisfying

$$\tau_{ij} = \mu \left(\frac{\partial U_i}{\partial x_j} + \frac{\partial U_j}{\partial x_i} - \frac{2}{3} \delta_{ij} \frac{\partial U_k}{\partial x_k} \right) \quad (3)$$

where δ_{ij} is Kronecker delta. If $i = j$, $\delta_{ij} = 1$; otherwise $\delta_{ij} = 0$. μ is the viscosity coefficient.

For the convenience of calculation, we use the nondimensional form of each variable:

$$t = \frac{\bar{t} u_\infty}{L}, x_i = \frac{\bar{x}_i}{L}, \rho = \frac{\rho}{\rho_\infty}, p = \frac{\bar{p}}{\rho_\infty u_\infty^2}$$

$$u_i = \frac{\bar{u}_i}{u_\infty}, \text{Re} = \frac{u_\infty L}{\nu_\infty}, g_i = \frac{\bar{g}_i}{u_\infty^2}, \nu = \frac{\bar{\nu}}{\nu_\infty}$$

In the finite element calculation, we discretize the equation in the time direction Codina et al. (1998). Then Eq. (2) can be inferred as follows.

$$\frac{U_i^{n+1} - U_i^n}{\Delta t} = -\frac{\partial}{\partial x_j} (u_j U_i)^n + \frac{\partial \tau_{ij}^n}{\partial x_j} - \frac{\partial p^{n+\theta}}{\partial x_i} + Q_i^n$$

$$+ \left(\frac{\Delta t}{2} u_k \frac{\partial}{\partial x_k} \left(\frac{\partial}{\partial x_j} (u_j U_i) - \frac{\partial p}{\partial x_i} + Q_i \right) \right)^n \quad (4)$$

where $p^{n+\theta}$ represents the pressure value at time $t = t^n + \theta \Delta t$. Δt represents the time step and $\theta \in (0, 1)$. It further follows that

$$\frac{\partial p^{n+\theta}}{\partial x_i} = \theta \frac{\partial p^{n+1}}{\partial x_i} + (1 - \theta) \frac{\partial p^n}{\partial x_i}$$

$$\frac{\partial p^{n-\theta}}{\partial x_i} = \theta \frac{\partial p^{n-1}}{\partial x_i} + (1 - \theta) \frac{\partial p^n}{\partial x_i} \quad (5)$$

At this stage we use CBS algorithm Zienkiewicz, Taylor and Nithiarasu (2014) to substitute a suitable approximation so that the calculation can be performed before p^{n+1} is obtained.

Using the auxiliary variables ΔU_i^* and ΔU_i^{**} we split Eq. (4) into two parts

$$\frac{U_i^{n+1} - U_i^n}{\Delta t} = \frac{\Delta U_i^*}{\Delta t} + \frac{\Delta U_i^{**}}{\Delta t} \quad (6)$$

$$\frac{\Delta U_i^*}{\Delta t} = -\frac{\partial}{\partial x_j} (u_j U_i)^n + \frac{\partial \tau_{ij}^n}{\partial x_j} + Q_i^n$$

$$+ \left(\frac{\Delta t}{2} u_k \frac{\partial}{\partial x_k} \left(\frac{\partial}{\partial x_j} (u_j U_i) + Q_i \right) \right)^n \quad (7)$$

$$\frac{\Delta U_i^{**}}{\Delta t} = -\frac{\partial p^{n+\theta_2}}{\partial x_i} + \frac{\Delta t}{2} u_k \frac{\partial^2 p^n}{\partial x_k \partial x_i} \quad (8)$$

Eq. (7) is solved by an explicit time step applied to the discretized form. Eq. (8) is obtained once $\Delta p = p^{n+1} - p^n$ is evaluated. From Eq. (1), we have

$$\frac{\Delta p}{\Delta t} = \frac{1}{c^2} \frac{\Delta p}{\Delta t} = -\frac{\partial U_i^{n+\theta_1}}{\partial x_i} = -\left[\frac{\partial U_i^n}{\partial x_i} + \theta_1 \frac{\partial \Delta U_i}{\partial x_i} \right] \quad (9)$$

Replacing ΔU_i by ΔU_i^* , using Eq. (6) and Eq. (8) and rearranging and neglecting third- and higher-order terms, we obtain

$$\frac{\Delta p}{\Delta t} = \frac{1}{c^2} \frac{\Delta p}{\Delta t} = -\frac{\partial U_i^n}{\partial x_i} - \theta_1 \frac{\partial \Delta U_i^*}{\partial x_i} + \Delta t \theta_1 \frac{\partial^2 p^{n+\theta_2}}{\partial x_i \partial x_i} \quad (10)$$

In the above equations, $0.5 \leq \theta_1 \leq 1.0$ and $\theta_2 = 0$ for explicit scheme, and $0.5 \leq \theta_1 \leq 1.0$ and $0.5 \leq \theta_2 \leq 1.0$ for semi-implicit scheme. In the following calculation process, we choosed semi-implicit scheme, and $\theta_1 = \theta_2 = 0.5$. The governing equations can be solved after spatial discretization in the following order:

- Step 1: use Eq. (7) to obtain ΔU_i^* .
- Step 2: use Eq. (10) to obtain Δp .
- Step 3: use Eq. (8) to obtain ΔU_i^{**} thus establishing the values of U_i and p .

After completing the calculation to establish ΔU_i and Δp , the transport equation is dealt with independently which we discuss in section 3.3.

CBS is initially used in the finite element method, so it retains the second order accuracy in the calculation process. Higher order accuracy is not impossible for neural networks, but the amount of calculation will increase exponentially. The second order accuracy has been proved to be accurate enough in the finite difference method Shankar and Deshpande (2000), so there is no higher order CBS algorithm derived here.

2.2. Cbs based PINN method

A PINN is essentially a DNN that can be used to approximate the solution determined by the data and PDEs. A residual neural network can be expressed as

$$(\mathbf{u}, p) = F_{NN}(\mathbf{x}, t; \Theta) \quad (11)$$

where F_{NN} represents the neural network, whose inputs are space coordinates $\mathbf{x} = (x_1, x_2, x_3)$ and time t . The parameter Θ represents the trainable variables. The outputs of the neural network are velocity vector $\mathbf{u} = (u_1, u_2, u_3)$ and pressure p . We set up separate networks for each output and use independent optimizer and learning rate for each network. In the process of selecting sampling points, we think the sampling points should meet certain requirements. In the finite element method, there must be at least ten points in a wavelength to correctly describe the waveform without divergence. Random sampling does not necessarily ensure that convergence requirements are satisfied everywhere in the space. If the random sampling result causes divergence, it will be better to fix the sampling points. The examples selected in the following sections are all in two-dimensional rectangular space, so the sampling points are selected as the structured grid. In fact, the unstructured mesh in the finite element method can also be selected as the sampling points. The time interval Δt is fixed. The calculation steps are as follows:

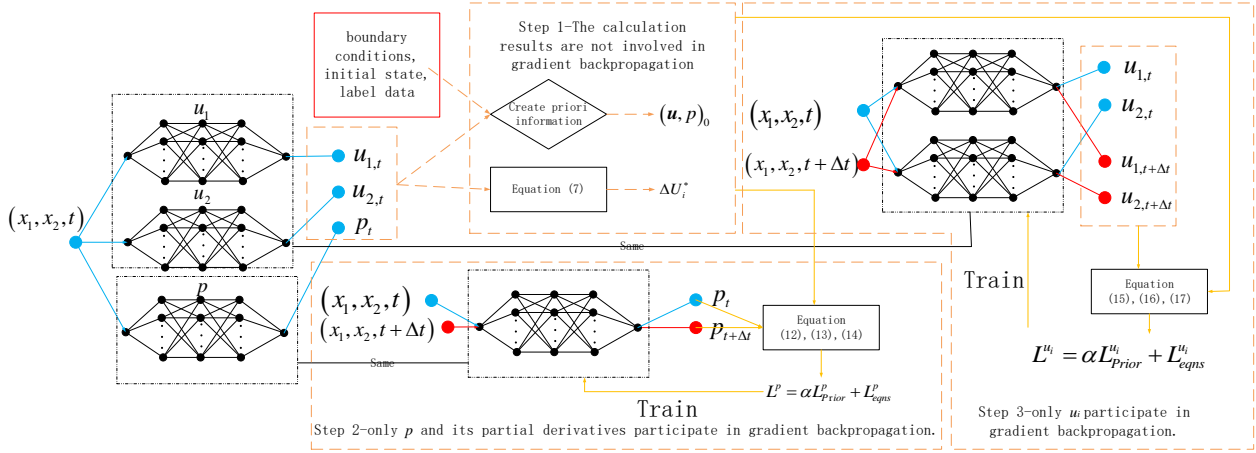


Figure 2: PINN based on CBS.

Step 1,

Use input N sampling points $(\mathbf{x}, t)^j$ to obtain the initial output $(\mathbf{u}, p)_b^j$. ΔU_i^* can be calculated by Eq. (7). We think that $(\mathbf{u}, t)_b^j$ should be regarded as prior information like the boundary conditions, initial state and label data. So we combine $(\mathbf{u}, t)_b^j$, boundary conditions, initial state and label data together to construct prior information $(\mathbf{u}, p)_0^j$. The construction method is to replace the original output point with the boundary conditions, initial state and label data.

Step 2,

Use input N sampling points $(\mathbf{x}, t + \Delta t)^j$ to obtain p_a^j . Δp_a^j can be calculated by Eq. (10). To make the network satisfy the governing equations, the loss function in the p 's network is defined as follows:

$$L^p = \alpha^p L_{Prior}^p + L_{eqns}^p \quad (12)$$

where α^p is a weighting coefficient. L_{Prior}^p and L_{eqns}^p are computed as

$$L_{Prior}^p = \sum_{j=1}^N (p_0^j - p_b^j)^2 / \Delta t^2 \quad (13)$$

$$L_{eqns}^p = \sum_{j=1}^N (p_a^j - p_0^j - \Delta p_a^j)^2 / \Delta t^2 \quad (14)$$

Here, L_{Prior}^p represents the loss between the prior information and the predicted data and L_{eqns}^p denotes the total residual of the N-S equations. Note that we use p_0 instead of p_b as the target result. This is also a common practice in the finite element method. Boundary conditions or known conditions replace the original data in the calculation process rather than after the calculation, which can obtain higher accuracy. Note that only p_a and its partial derivatives participate in gradient backpropagation.

Repeat Step 2 for K^p times and recalculate Δp_a^j .

Step 3,

Use input N sampling points $(\mathbf{x}, t + \Delta t)^j$ to obtain $u_{i,a}^j$. $\Delta U_{i,a}^j$ can be calculated by Eq. (8). ρ_0 and ρ_a can be calculated by Eq. (10). The loss function in the u_i 's network is defined as follows:

$$L^{u_i} = \alpha^{u_i} L_{Prior}^{u_i} + L_{eqns}^{u_i} \quad (15)$$

where α^{u_i} is a weighting coefficient, and $L_{Prior}^{u_i}$ and $L_{eqns}^{u_i}$ are computed as

$$L_{Prior}^{u_i} = \sum_{j=1}^N (u_{i,0}^j - u_{i,b}^j)^2 / \Delta t^2 \quad (16)$$

$$L_{eqns}^{u_i} = \sum_{j=1}^N (u_{i,a}^j - (\rho_0 u_{i,0}^j + \Delta U_{i,a}^j) / \rho_a)^2 / \Delta t^2 \quad (17)$$

Here, $L_{Prior}^{u_i}$ represents the loss between the prior information and the predicted data, and $L_{eqns}^{u_i}$ denotes the total residual of the N-S equations. Note that only $u_{i,a}$ participate in gradient backpropagation.

Repeat Step 3 for K^{u_i} times and retain $\Delta U_{i,a}^j$.

Repeat Step 1-3 until L convergences to required accuracy, shown in Fig. 2. It can be seen that each input point in each step has two reference data: one is the prior information I_0 , and the other is the posterior information I_1 obtained from Eq. (1)-(2). So theoretically, the final output result of each step will converge to $I_{final} = (I_1 + \alpha I_0) / (1 + \alpha)$. And the final loss L_{final} has a relationship with the initial loss L_{init} as $L_{final} \geq \frac{\alpha}{(1+\alpha)} L_{init}$. So when loss decreases by $\frac{1}{2(1+\alpha)} L_{init}$, it is unnecessary to increase K . When α decreases, the convergence speed will accelerate, but it is easy to diverge. When output continues to diverge, the corresponding α should be increased. α should be set to a larger value at first to prevent divergence, and α should

be adjusted to a smaller value after stabilizing to speed up convergence. As α will change during commissioning, the values of α mentioned below will be the last set values.

It should be pointed out that the theoretical convergence result of this method does not depend on the network structure. When the network can fit the results with the required accuracy, changing the network structure will only affect the convergence rate. So all the networks mentioned below have the same network structure: the number of hidden layers $N_{layer} = 6$, the number of neurons $N_{cell} = 128$ in each hidden layer and the activation function is swish function $\sigma(x) = \frac{x}{1+e^{-x}}$. In order to compute the residuals of the N-S equations, the partial differential operators are computed by using automatic differentiation (AD), which can be directly formulated in the deep learning framework, e.g., using “torch.autograd.grad” in Torch. In AD, the derivatives in the governing equations are approximated by the derivatives of the output with respect to the input of the PINNs. Use “with torch.no_grad()” to indicates that the current calculation does not need backpropagation.

The following is divided into two parts: 1. Use the shallow-water equations to solve the solitary wave problem, and it is pointed out that the separation of output parameters is more suitable for practical engineering applications; and 2. Solve the incompressible N-S equations with exact solutions and prove the method’s correctness and universality.

3. Shallow Water Problems

The isothermal compressible flow equations can be transformed into the depth integrated shallow-water equations with the variables being changed as follows:

$$\begin{aligned}\rho(\text{density}) &\rightarrow h(\text{depth}) \\ u_i(\text{velocity}) &\rightarrow \bar{u}_i(\text{mean-velocity}) \\ p(\text{pressure}) &\rightarrow \frac{1}{2}g(h^2 - H^2)\end{aligned}$$

It can be written in a convenient form for the general CBS formulation as

$$\frac{\partial h}{\partial t} + \frac{\partial U_i}{\partial x_i} = 0 \quad (18)$$

$$\frac{\partial U_i}{\partial t} + \frac{\partial (\bar{u}_j U_i)}{\partial x_j} + \frac{\partial}{\partial x_i} \left(\frac{1}{2}g(h^2 - H^2) \right) + Q_i = 0 \quad (19)$$

where $U_i = h\bar{u}_i$, and H is the mean-depth. The rest of the variables are the same as those described before. Set $Q_i = 0$. The three essential steps of the CBS scheme can be written in its semi-discrete form as

Step 1,

$$\Delta U_{i,a}^* = \Delta t \left[-\frac{\partial (\bar{u}_j U_i)}{\partial x_j} + \frac{\Delta t}{2} u_k \frac{\partial}{\partial x_i} \left(\frac{\partial (\bar{u}_j U_i)}{\partial x_j} \right) \right]^n \quad (20)$$

Step 2,

$$\Delta h_a = -\Delta t \left[\frac{\partial (U_i^n)}{\partial x_j} + \theta_1 \frac{\partial \Delta U_i^*}{\partial x_i} - \Delta t \theta_1 \frac{\partial^2 p^{n+\theta_2}}{\partial x_i \partial x_i} \right] \quad (21)$$

$$L_{Prior}^h = \sum_{j=1}^N (h_0 - h_b)^2 / \Delta t^2 \quad (22)$$

$$L_{eqns}^h = \sum_{j=1}^N (h_a - h_0 - \Delta h_a)^2 / \Delta t^2 \quad (23)$$

Step 3,

$$\Delta U_{i,a} = \Delta U_{i,a}^* - \Delta t \frac{\partial p_i^{n+\theta_2}}{\partial x_i} + \frac{\Delta t^2}{2} \bar{u}_k \frac{\partial^2 p^n}{\partial x_k \partial x_i} \quad (24)$$

$$L_{Prior}^{u_i} = \sum_{j=1}^N (u_{i,0}^j - u_{i,b}^j)^2 / \Delta t^2 \quad (25)$$

$$L_{eqns}^{u_i} = \sum_{j=1}^N (u_{i,a}^j - (h_0 u_{i,0}^j + \Delta U_{i,a}^j) / h_a)^2 / \Delta t^2 \quad (26)$$

with $p = g(h^2 - H^2)$.

The propagation process of solitary wave in a flat-bottomed flume has an accurate solution, which can be used to verify the correctness of the method. The wave height and velocity of solitary waves do not change in the propagation process in the flat-bottomed flume. In order to make the problem more complex, we calculate solitary wave’s propagation process onto a shelving beach, shown in Fig. 3. Solitary wave’s propagation process Löhner, Morgan and Zienkiewicz (1984) can be approximately expressed as:

$$\begin{aligned}\eta(x_1, x_2, t) &= \text{asech}^2 \left(\sqrt{3a/4h^3} \times (x_1 - 30 - Ct) \right) \\ u_1(x_1, x_2, t) &= -(l + 1/2a)\eta / ((x_1 - Ct)/30 + \eta)\end{aligned} \quad (27)$$

with $u_2(x, y, t) = 0$ and $C = \sqrt{gh(1 + H/h)}$. Set $g = 1.0$, so $C \approx 1.0$. It should be pointed out that the above equation is its approximate expression. But regardless of whether the equation is correct or not, this method can always derive the solution that meets the priori information and shallow-water equations.

3.1. Solve when the initial state is known

The computation is carried out in the domain of $0 \leq x_1 \leq 40$, $0 \leq x_2 \leq 5$ and $0 \leq t \leq 10$. Sampling interval is $\Delta x_1 = 0.25$, $\Delta x_2 = 0.25$ and $\Delta t = 0.125$. So the total number of sampling points is $N = 161 * 21 * 81 = 273861$. All three networks use the Adam optimizer

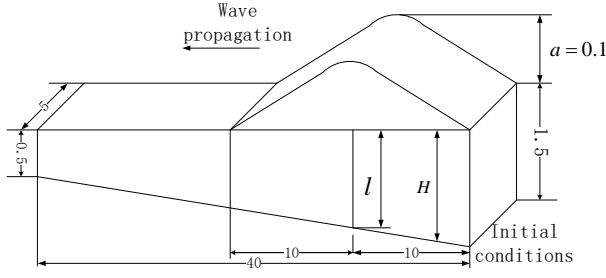


Figure 3: Solitary wave in the inclined bottom flume.

and $\alpha^p = \alpha^{u_1} = \alpha^{u_2} = 1$. The initial state equations and boundary conditions are

$$\eta(x_1, x_2, 0) = \text{asech}^2 \left(\sqrt{3a/4h^3} \times (x_1 - 30) \right) \quad (28)$$

$$u_1(x_1, x_2, 0) = -(l + 1/2a) \eta / (x_1/30 + \eta)$$

$$\begin{cases} u_1(0, x_2, t) = 0, u_1(40, x_2, t) = 0 \\ u_2(x_1, 0, t) = 0, u_2(x_1, 5, t) = 0 \end{cases} \quad (29)$$

The pseudo code of the calculation process is as follows:

Algorithm 1 shallow-water problem

```

1: Set  $\Delta t = 0.125$ 
2: get  $h_{ini}, \bar{u}_{i,ini}$  by Eq. (28)
3: for step in range(1000) do
4:   //Step 1
5:   input N points  $(\mathbf{x}, t)$  to obtain  $\bar{u}_{i,b}, h_b$ 
6:   with torch.no_grad():  $\triangleright$  Create priori information
7:    $h_0, \bar{u}_{i,0} = \text{clone}(\bar{u}_{i,b}, h_b)$ 
8:    $h_0(:, t=0), \bar{u}_{i,0}(:, t=0) = h_{ini}, \bar{u}_{i,ini}$ 
9:    $\bar{u}_{1,0}(x_2 = 0, :) = \bar{u}_{1,0}(x_2 = 40, :) = 0$ 
10:   $\bar{u}_{2,0}(x_1 = 0, :) = \bar{u}_{2,0}(x_1 = 5, :) = 0$ 
11:  get  $\Delta U_{i,a}^*$  by Eq. (20).
12:  //Step 2
13:  with torch.no_grad():  $\triangleright$  Prepare for  $\Delta h_a$ 
14:  get  $\frac{\partial(U_i^n)}{\partial x_j}, \frac{\partial \Delta U_i^*}{\partial x_i}$  by AD
15:  for  $k$  in range( $K_h$ ) do
16:    input N points  $(\mathbf{x}, t)$  and  $(\mathbf{x}, t + \Delta t)$  to obtain  $h_b$ 
    and  $h_a$ , Respectively
17:    get  $\frac{\partial^2 p^{n+\theta_2}}{\partial x_i \partial x_j}$   $\triangleright$  Gradient is not mandatory
18:    get  $\Delta h_a$  by Eq. (21)
19:    get  $L^h$  by Eqs. (22),(23)
20:     $L^h.backward()$  and use Adam Optimizer
21:  end for
22:  //Step 3
23:  with torch.no_grad():
24:    input N points  $(\mathbf{x}, t + \Delta t)$  to obtain  $h_a$ 
25:    get  $\frac{\partial p_{i,a}}{\partial x_i}$ 
26:    get  $\Delta U_{i,a}$  by Eq. (24)
27:    for  $k$  in range( $K_{u_i}$ ) do

```

```

28:    input N points  $(\mathbf{x}, t)$  and  $(\mathbf{x}, t + \Delta t)$  to obtain  $\bar{u}_{i,b}$ 
    and  $\bar{u}_{i,a}$ , Respectively
29:    get  $L^{u_i}$  by Eqs. (25),(26)
30:     $L^{u_i}.backward()$  and use Adam Optimizer
31:  end for
32: end for

```

The initial state of u_2 is not given here, so the conditions for solving the equations are incomplete. However, the neural network still gives a solution, shown in Fig. 4. At the beginning, we thought that when the conditions were incomplete, the result would tend to be a steady solution without time term. But obviously, if the calculation continues, u_2 will tend to diverge. Therefore, the neural network can not go beyond the conventional method and give the correct answer under insufficient conditions.

Although u_2 does not tend to 0 as expected, solitary wave is still well described. The propagation speed is about 1.0, which is consistent with the expectation. At the same time, the wave height increases during the propagation process, which is also consistent with the theoretical results.

3.2. Solve when the intermediate state is known

In this chapter, we want to discuss how to obtain the past and the future information when the intermediate time information is known. The boundary conditions are the same as those in Eq. (29). The intermediate state equations are

$$\begin{aligned} \eta(x_1, x_2, 5) &= \text{asech}^2 \left(\sqrt{3a/4h^3} \times (x_1 - 25) \right) \\ u_1(x_1, x_2, 5) &= -(l + 1/2a) \eta / ((x_1 - 5)/30 + \eta) \\ u_2(x_1, x_2, 5) &= 0 \end{aligned} \quad (30)$$

In the previous process, the networks only obtain the future flow field information from the current flow field. We make the networks obtain the past flow field information by adding the time-step items as follows:

Step 1,

Calculate $\Delta U_{i,a}^*$ and $\Delta U_{i,c}^*$ by Eq. (7) and Eq. (31).

$$\Delta U_{i,c}^* =$$

$$\Delta t \left[-\frac{\partial(\bar{u}_j U_i)}{\partial x_j} + \frac{\Delta t}{2} u_k \frac{\partial}{\partial x_i} \left(\frac{\partial(\bar{u}_j U_i)}{\partial x_j} \right) \right]^n \quad (31)$$

Step 2,

Use input $(\mathbf{x}, t - \Delta t)^j$ to obtain h_c^j . Change L_{eqns}^h as

$$\begin{aligned} L_{eqns}^h &= \sum_{j=1}^N (h_a^j - h_0^j - \Delta h_a^j)^2 / \Delta t^2 \\ &+ \sum_{j=1}^N (h_c^j - h_0^j - \Delta h_c^j)^2 / \Delta t^2 \end{aligned} \quad (32)$$

Δh_c is computed as

$$\Delta h_c = \Delta t \left[\frac{\partial(U_i^n)}{\partial x_j} + \theta_1 \frac{\partial \Delta U_{i,a}^*}{\partial x_i} - \Delta t \theta_1 \frac{\partial^2 p^{n-\theta_2}}{\partial x_i \partial x_j} \right] \quad (33)$$

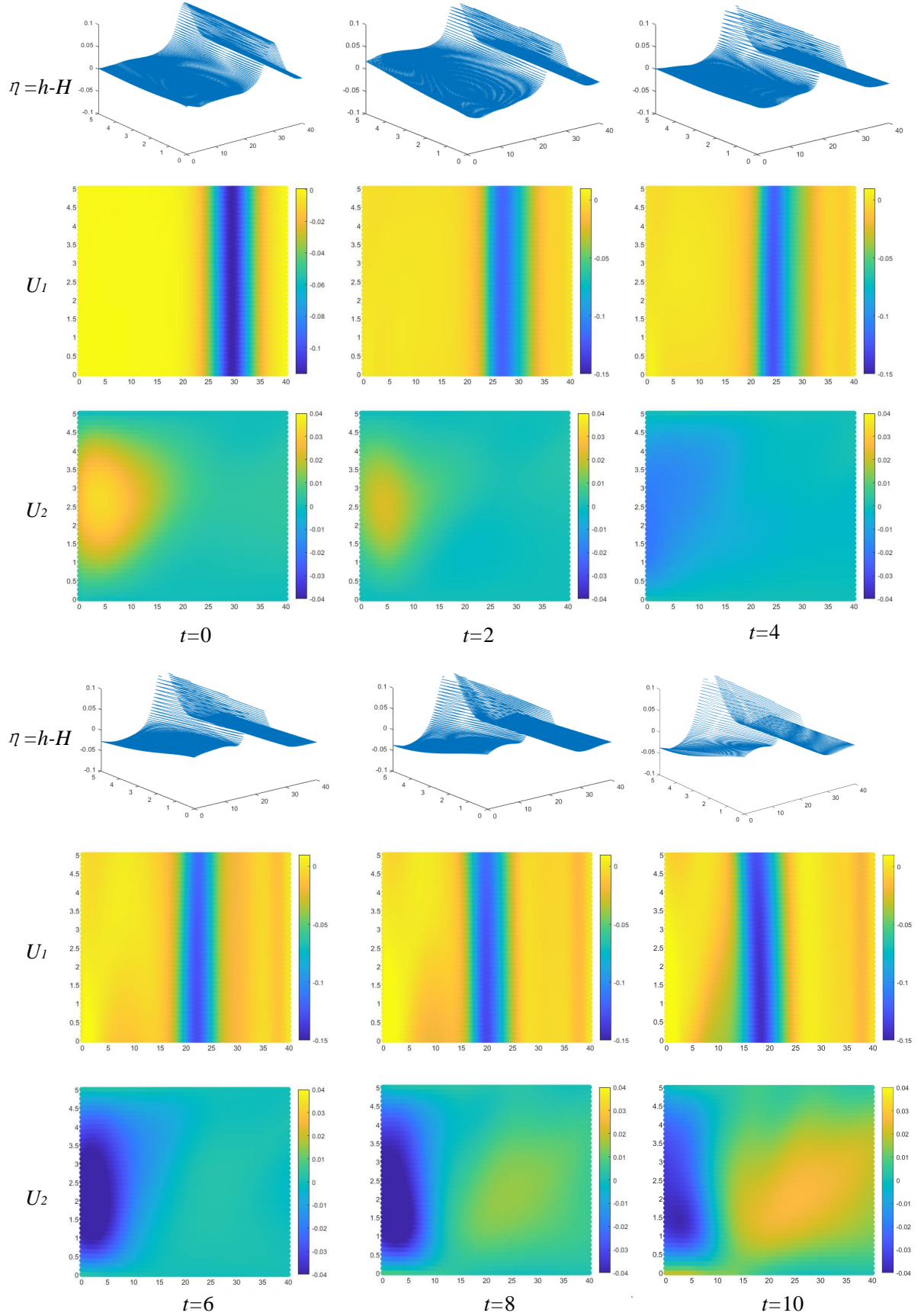


Figure 4: Solitary wave in the inclined bottom flume. Results with incomplete initial conditions.

Step 3,

Use input $(\mathbf{x}, t - \Delta t)^j$ to obtain $u_{i,c}^j$. Change $L_{eqns}^{u_i}$ as

$$L_{eqns}^{u_i} = \sum_{j=1}^N (u_{i,a}^j - (h_0 u_{i,0}^j + \Delta U_{i,a}^j) / h_a)^2 / \Delta t^2 + \sum_{j=1}^N (u_{i,c}^j - (h_0 u_{i,0}^j + \Delta U_{i,c}^j) / h_c)^2 / \Delta t^2 \quad (34)$$

$\Delta U_{i,c}$ is computed as

$$\Delta U_{i,c} = \Delta U_{i,c}^* + \Delta t \frac{\partial p_i^{n-\theta_2}}{\partial x_i} + \frac{\Delta t^2}{2} \bar{u}_k \frac{\partial^2 p^n}{\partial x_k \partial x_i} \quad (35)$$

When other settings remain unchanged, the above modifications can achieve better results, shown in Fig. 5. It can improve the stability of the results, but it also reduce the convergence speed. The finite element method itself implies many boundary conditions: parameters outside the calculation area do not exist. Mathematically, it and its partial derivatives of all orders are 0. This has both advantages and disadvantages. It does not need to set the boundary condition of the parameter partial derivative term. But it cannot deal with the reflection of the wave at the boundary. The parameters of the neural network outside the calculation area still exist. So when the wave flows out of the calculation area, it will not be reflected. But when faced with some problems, more boundary conditions are needed. The time-step-back items are added in the above method. The time-step-back and time-step items are considered at the same time, which to some extent has the effect that the partial derivatives of the boundary parameters are 0, and can replace some boundary conditions.

3.3. Shallow-water transport

In engineering applications, we often only need a part of the information to guide production. This is not cost-effective if every information acquisition requires a huge neural network to obtain all information. The separation of output parameters can solve this problem and make it more convenient for further calculation. We show how to calculate the dispersio of some quantities in the shallow-water when the flow field information is known.

From the flow field information obtained above, we can calculate some quantities' dispersion. The depth-averaged transport equation can be calculated in which the averaged velocities u have been determined independently. A typical averaged equation can be written as

$$\frac{\partial (hT)}{\partial t} + \frac{\partial (h\bar{u}_i T)}{\partial x_i} - \frac{\partial}{\partial x_i} \left(hk \frac{\partial T}{\partial x_i} \right) + R = 0 \quad (36)$$

Where h and \bar{u}_i are the previously defined and computed quantities, k is an appropriate diffusion coefficient, and R is a source term. Set $R = 0$. The application of the CBS method for any scalar transport equation is straightforward, because of the absence of the pressure gradient term. Now

a new time integration parameter θ_3 is introduced for the diffusion term such that $0 \leq \theta_3 \leq 1$. We used the method that considers both time-step and time-step-back items to reduce the boundary conditions. The form is:

$$\Delta h T_a = h T^{n+1} - h T^n = -\Delta t \left[\frac{\partial (h\bar{u}_i T_b)}{\partial x_i} - \frac{\Delta t}{2} u_k \frac{\partial}{\partial x_k} \left(\frac{\partial (h\bar{u}_i T_b)}{\partial x_i} \right) \right]^n + \Delta t \frac{\partial}{\partial x_i} \left(hk \frac{\partial T^{n+\theta_3}}{\partial x_i} \right) \quad (37)$$

$$\Delta h T_c = h T^{n-1} - h T^n = \Delta t \left[\frac{\partial (h\bar{u}_i T_b)}{\partial x_i} + \frac{\Delta t}{2} u_k \frac{\partial}{\partial x_k} \left(\frac{\partial (h\bar{u}_i T_b)}{\partial x_i} \right) \right]^n - \Delta t \frac{\partial}{\partial x_i} \left(hk \frac{\partial T^{n-\theta_3}}{\partial x_i} \right) \quad (38)$$

$$L_{eqns}^T = \sum_{j=1}^N \left(T_a^j - (h_0 T_0^j + \Delta h T_a^j) / h_a \right)^2 / \Delta t^2 + \sum_{j=1}^N \left(T_c^j - (h_0 T_0^j + \Delta h T_c^j) / h_c \right)^2 / \Delta t^2 \quad (39)$$

The computation is carried out in the domain of $20 \leq x_1 \leq 25$, $0 \leq x_2 \leq 5$ and $0 \leq t \leq 10$. Sampling interval is $\Delta x_1 = 0.25$, $\Delta x_2 = 0.25$ and $\Delta t = 0.125$. So the total number of sampling points is $N = 21 * 21 * 81 = 35721$. The network use the Adam optimizer and $\alpha^T = 10$. The initial state equation is

$$T(x, y, 0) = \frac{10}{\sqrt{2\pi}} \exp \left(-((x - 22.5)^2 + (y - 2.5)^2) / 2 \right) \quad (40)$$

The pseudo code of the calculation process is as follows:

Algorithm 2 shallow-water transport problem

- 1: Set $\Delta t = 0.125$
 - 2: get T_{ini} by Eq. (40)
 - 3: **for** step in range(1000) **do**
 - 4: input N points (\mathbf{x}, t) to obtain \bar{u}_i, h and T_b
 - 5: with torch.no_grad(): ▷ Create priori information
 - 6: $T_0 = clone(T_b)$
 - 7: $T_0(:, t = 0) = T_{ini}$
 - 8: **for** k in range(K_T) **do**
 - 9: input N points (\mathbf{x}, t) , $(\mathbf{x}, t + \Delta t)$ and $(\mathbf{x}, t - \Delta t)$ to obtain T_b, T_a and T_c , Respectively
 - 10: with torch.no_grad():
 - 11: get $\Delta h T_a$ and $\Delta h T_c$ by Eqs. (37),(38)
 - 12: get L_{eqns}^T by Eqs. (39)
 - 13: $L^T.backward()$ and use Adam Optimizer
 - 14: **end for**
 - 15: **end for**
-

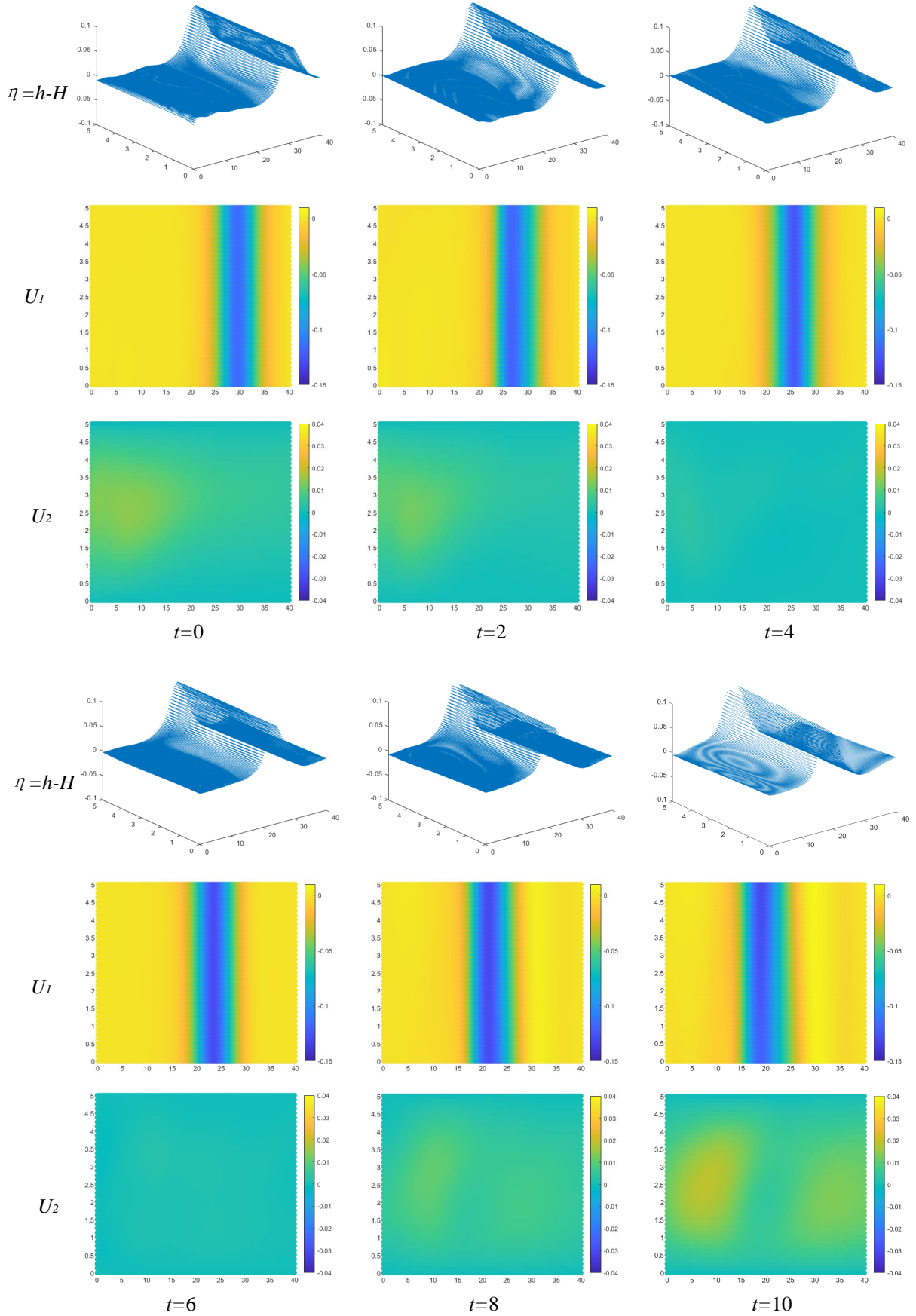


Figure 5: Solitary wave in the inclined bottom flume. Results with complete intermediate conditions.

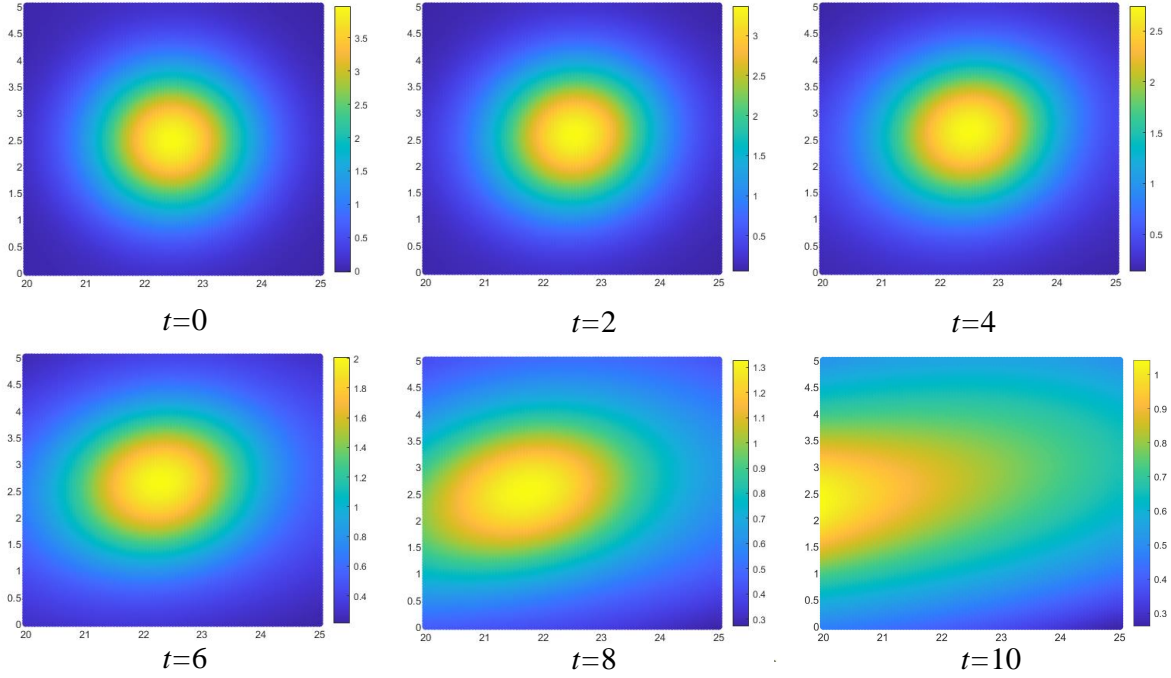


Figure 6: Temperature field.

Stable results can be obtained without boundary conditions, shown in Fig. 6. The temperature field shifts to the right due to the flow field, and the temperature decreases due to diffusion.

4. Incompressible Flow

As we said in section 3, the shallow water flow equation is a N-S equations' deformation, and the incompressible flow is also an N-S equations' special case. When we discuss incompressible flow, we think that $c \rightarrow \infty$, and Eq. (1) becomes

$$0 = -\frac{\partial u_i}{\partial x_i} \quad (41)$$

Momentum conservation

$$\frac{\partial u_i}{\partial t} = -\frac{\partial}{\partial x_j} (u_j u_i) + \frac{1}{\text{Re}} \frac{\partial^2 u_i}{\partial x_i^2} - \frac{\partial p}{\partial x_i} \quad (42)$$

Where Re represents the Reynolds number. The rest of the variables are the same as those described before. Obviously, such simplification leads to the pressure information loss. The change of p is affected by the current flow field. Water is generally considered as an incompressible flow, and its sound velocity is $c = 1480 \text{ m/s}$. In the finite element method, there are two ways to deal with it. One is to retain the p item in the mass formula, so the time accuracy will become extremely high. If the mesh size is $dx = 0.1 \text{ m}$, then the time step should meet the requirement $\Delta t = 0.1/1480 \text{ s}$. The other

is to use the implicit scheme like CBS. The three essential steps of the CBS scheme can be written in its semi-discrete form as

Step 1,

$$\Delta u_{i,a}^* = \Delta t \left[-\frac{\partial (u_j u_i)}{\partial x_j} + \frac{\Delta t}{2} u_k \frac{\partial}{\partial x_i} \left(\frac{\partial (u_j u_i)}{\partial x_j} \right) + \frac{1}{\text{Re}} \frac{\partial^2 u_i}{\partial x_i^2} \right]^n \quad (43)$$

Step 2,

$$\Delta_a = \Delta t \left[\frac{\partial (u_i^n)}{\partial x_j} + \theta_1 \frac{\partial \Delta u_{i,a}^*}{\partial x_i} + \Delta t \theta_1 \frac{\partial^2 p^{n+\theta_2}}{\partial x_i \partial x_i} \right] \quad (44)$$

$$L_{\text{Prior}}^p = \sum_{j=1}^N (p_0^j - p_b^j)^2 / \Delta t^2 \quad (45)$$

$$L_{\text{eqns}}^p = \sum_{j=1}^N (\Delta_a)^2 / \Delta t^2 \quad (46)$$

Step 3,

$$\Delta u_{i,a} = \Delta u_{i,a}^* - \Delta t \frac{\partial p_i^{n+\theta_2}}{\partial x_i} + \frac{\Delta t^2}{2} u_k \frac{\partial^2 p^n}{\partial x_k \partial x_i} \quad (47)$$

$$L_{\text{Prior}}^{u_i} = \sum_{j=1}^N (u_{i,0}^j - u_{i,b}^j)^2 / \Delta t^2 \quad (48)$$

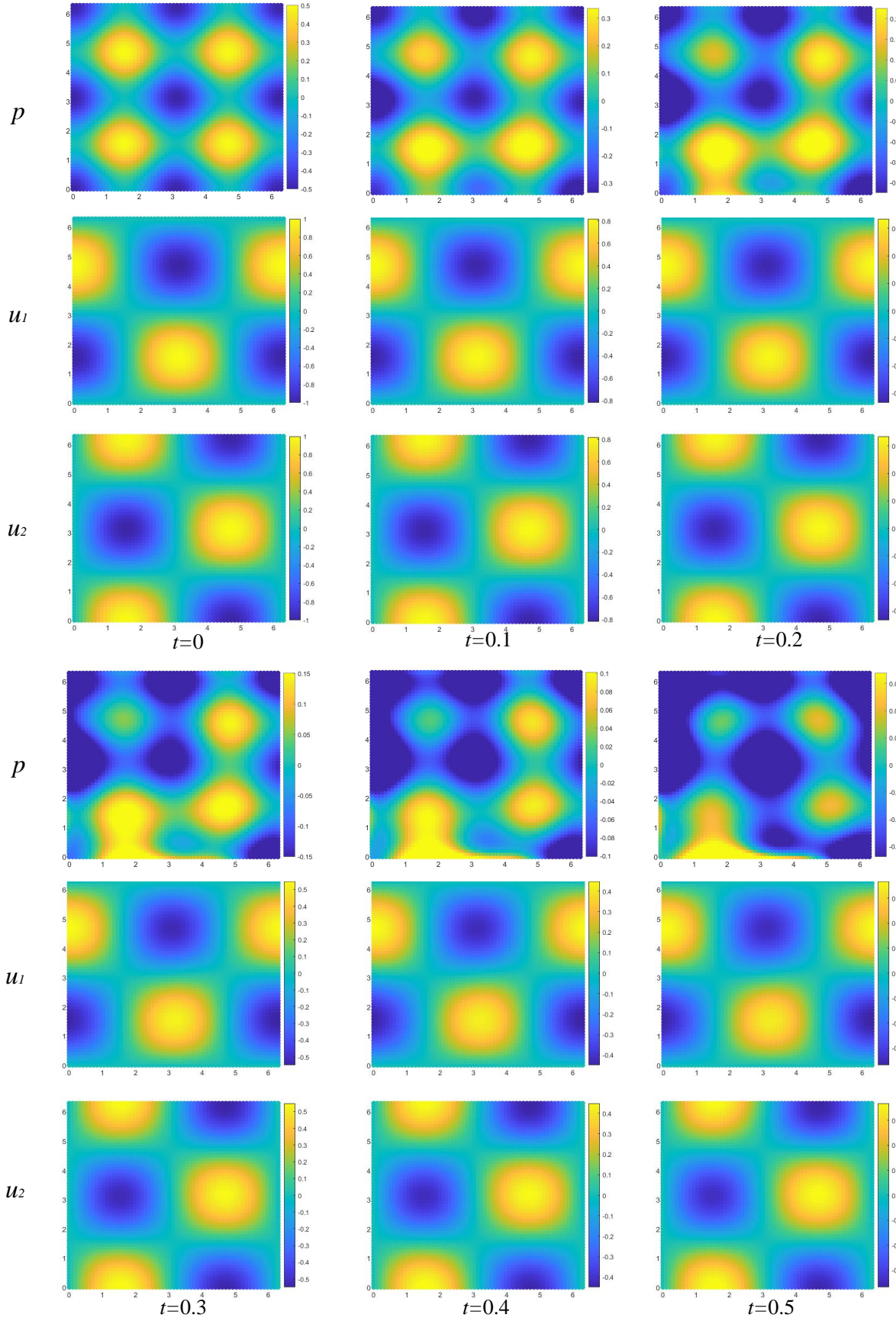


Figure 7: The spatial distribution of p , u_1 and u_2 from top to bottom. From left to right is their change with time. Boundary conditions without p .

$$L_{eqns}^{u_i} = \sum_{j=1}^N \left(u_{i,a}^j - u_{i,0}^j - \Delta u_{i,a}^j \right)^2 / \Delta t^2 \quad (49)$$

We consider 2D Taylor's decaying vortices to check the method. When $Re = 1$, an exact solution to Eqs. (41)-(42) given by F.R.S. (1923) is as follows:

$$\begin{aligned} u_1(x_1, x_2, t) &= -\cos(x_1) \sin(x_2) e^{-2t} \\ u_2(x_1, x_2, t) &= \sin(x_1) \cos(x_2) e^{-2t} \\ p(x_1, x_2, t) &= -0.25 (\cos(2x_1) + \cos(2x_2)) e^{-4t} \end{aligned} \quad (50)$$

The computation is carried out in the domain of $0 \leq x_1 \leq 2\pi$, $0 \leq x_2 \leq 2\pi$ and $0 \leq t \leq 2$. Sampling interval is $\Delta x_1 = 0.05\pi$, $\Delta x_2 = 0.05\pi$ and $\Delta t = 0.025$. So the total number of sampling points is $N = 41 * 41 * 21 = 35301$. All three networks use the Adam optimizer and $\alpha^p = 0.01$, $\alpha^{u_1} = \alpha^{u_2} = 0.1$. The initial state equations and boundary conditions are

$$\begin{aligned} u_1(x_1, x_2, 0) &= -\cos(x_1) \sin(x_2) \\ u_2(x_1, x_2, 0) &= \sin(x_1) \cos(x_2) \\ p(x_1, x_2, 0) &= -0.25 (\cos(2x_1) + \cos(2x_2)) \end{aligned} \quad (51)$$

$$\begin{cases} u_1(0, x_2, t) = u_1(2\pi, x_2, t) = -\sin(x_2) \\ u_1(x_2, 0, t) = u_1(x_1, 2\pi, t) = 0 \\ u_2(0, x_2, t) = u_2(2\pi, x_2, t) = 0 \\ u_2(x_1, 0, t) = u_2(x_1, 2\pi, t) = \sin(x_1) \end{cases} \quad (52)$$

The results are shown in Fig. 7. It can be seen that the results of u_1 and u_2 are more consistent with the exact solution, while p has a large deviation from the exact solution. It can be seen that p has a large leakage at the boundary

In order to get the correct results, additional boundary conditions about pressure need to be added as

$$\begin{cases} p(0, x_2, t) = p(2\pi, x_2, t) = -0.25(1 + \cos(2x_2)) \\ p(x_1, 0, t) = p(x_1, 2\pi, t) = -0.25(1 + \cos(2x_1)) \end{cases} \quad (53)$$

A classical problem - closed cavity driven by the motion of a lid (Shankar and Deshpande, 2000)- can explain why more boundary conditions are needed, shown in Fig. 8. The result shows that the velocity component, which is parallel to the wall, has a great impact on the overall flow field, which shows the role of the viscous item. There are no parameters outside the calculation domain in the finite element method, and the values on the boundarys are only affected by the parameters in the calculation domain. However, in the neural networks, the parameters outside the calculation domain can continuously affect the values on the boundary. This is like applying random parallel wall velocity components to the four walls in a cavity. So the neural networks need more boundary conditions to limit the results, and the finite element method can omit some boundary conditions when dealing with some symmetric problems.

The pseudo code of the calculation process is as follows:

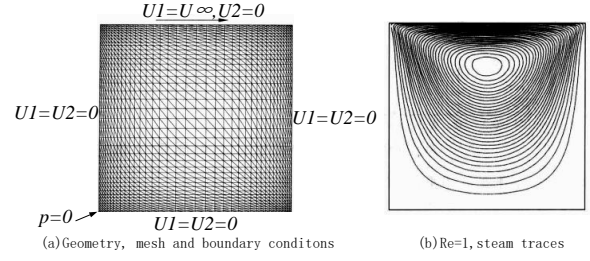


Figure 8: Incompressible flow in a lid-driven cavity. (a) Geometry, mesh and boundary conditions; (b) $Re=1$, steam traces.

Algorithm 3 Incompressible N-S equations problem

```

1: Set  $\Delta t = 0.005$ 
2: get  $p_{ini}, u_{i,ini}$  by Eq. (28)
3: for step in range(1000) do
4:   //Step 1
5:   input N points  $(\mathbf{x}, t)$  to obtain  $\bar{u}_{i,b}, h_b$ 
6:   with torch.no_grad():  $\triangleright$  Create priori information
7:      $u_{i,0}, p_0 = clone(u_{i,b}, p_b)$ 
8:      $p_0(\cdot, t=0), u_{i,0}(\cdot, t=0) = p_{ini}, u_{i,ini}$ 
9:     add boundary conditions by Eqs. (52),(53)
10:    get  $\Delta u_{i,a}^*$  by Eq. (43).
11:    //Step 2
12:    with torch.no_grad():  $\triangleright$  Prepare for  $\Delta p_a$ 
13:      get  $\frac{\partial(u_i^n)}{\partial x_j}, \frac{\partial \Delta u_i^*}{\partial x_i}$  by AD
14:      for  $k$  in range( $K_p$ ) do
15:        input N points  $(\mathbf{x}, t)$  and  $(\mathbf{x}, t + \Delta t)$  to obtain  $p_b$ 
        and  $p_a$ , Respectively
16:        get  $\frac{\partial^2 p^{n+\theta_2}}{\partial x_i \partial x_i}$   $\triangleright$  Gradient is mandatory
17:        get  $\Delta_a$  by Eq. (44)
18:        get  $L^p$  by Eqs. (45),(46)
19:         $L^p.backward()$  and use Adam Optimizer
20:      end for
21:      //Step 3
22:      with torch.no_grad():
23:        input N points  $(\mathbf{x}, t + \Delta t)$  to obtain  $p_a$ 
24:        get  $\frac{\partial p_{i,a}}{\partial x_i}$ 
25:        get  $\Delta u_{i,a}$  by Eq. (47)
26:        for  $k$  in range( $K_{u_i}$ ) do
27:          input N points  $(\mathbf{x}, t)$  and  $(\mathbf{x}, t + \Delta t)$  to obtain  $u_{i,b}$ 
          and  $u_{i,a}$ , Respectively
28:          get  $L^{u_i}$  by Eqs. (48),(49)
29:           $L^{u_i}.backward()$  and use Adam Optimizer
30:        end for
31:      end for

```

Set $\alpha^p = 0.001$, $\alpha^{u_1} = \alpha^{u_2} = 10$ and other conditions remain unchanged. The results with Eq. (53) are shown in Fig. 9. The L_2 norm can be used to evaluate the accuracy of the results. L_2 norm of p , u_1 and u_2 are 0.17, 0.017 and 0.015 respectively. Relative to u_1 and u_2 , p is a high-frequency variable. F-principle is well reflected here. At this

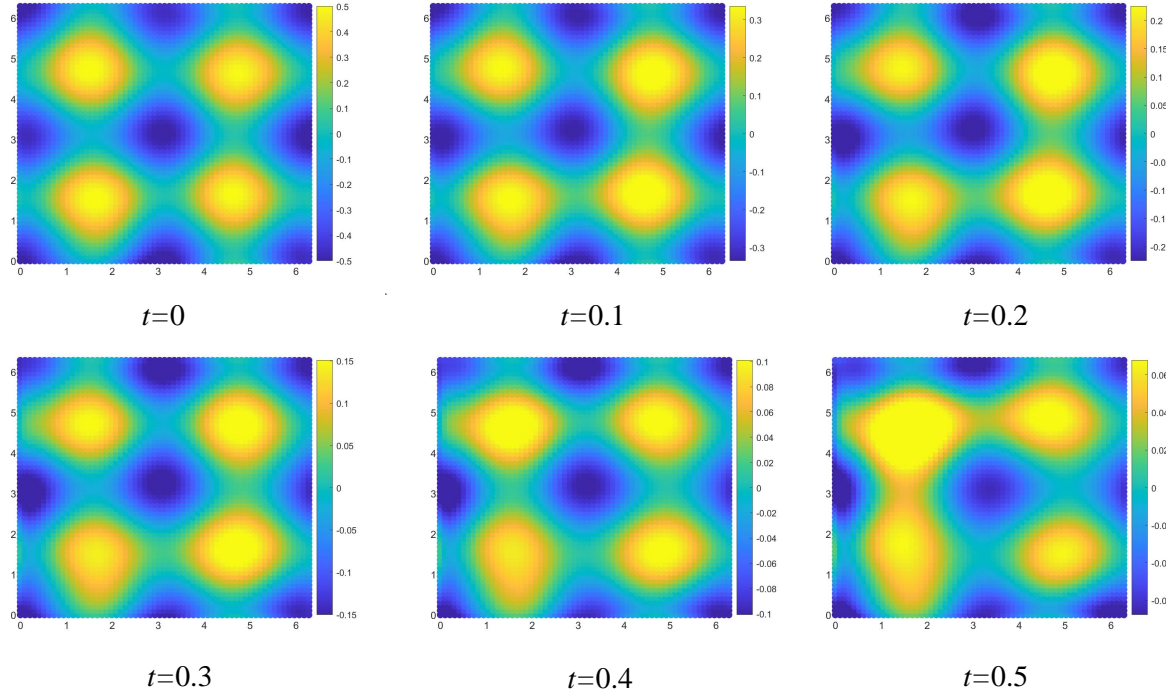


Figure 9: The spatial distribution of p . From left to right is their change with time. Boundary conditions with p . $\Delta t = 0.0125$

time, the simplest way is to reduce the time step Δt . When $\Delta t = 0.005$ and other conditions remain unchanged, L_2 norm of p , u_1 and u_2 can be reduced to 0.13, 0.0069 and 0.0071 respectively, shown in Fig. 10.

5. Conclusions

This paper proposes a PINN method based on CBS. This method can be used to solve the special form of compressible N-S equations - Shallow-Water equations, and incompressible N-S equations. It is a fast version for it does not need to consider the weights between output parameters and not all partial derivatives participate in gradient backpropagation. We study at least how many conditions are needed to make the network output a reliable and stable solution. We also discuss when and why this method need more strict conditions than the finite element method. We believe that the reason that limits the ability of PINN to solve PDEs is not the network itself, but the algorithm used by the network. Like the finite element method, the neural network is only a spatiotemporal approximation method, which requires corresponding algorithms to explore its performance. Although the solution speed of neural network method is slower than that of traditional methods such as the finite element method. In terms of theoretical accuracy, we believe that our neural network method can achieve higher accuracy by improving the accuracy of the algorithm, compared with the finite element method. And we believe that the separation of output parameters is more suitable for practical engineering

applications, compared with other fully connected PINN methods.

References

- Amini Niaki, S., Haghighat, E., Campbell, T., Poursartip, A., Vaziri, R., 2021. Physics-informed neural network for modelling the thermochemical curing process of composite-tool systems during manufacture. *Computer Methods in Applied Mechanics and Engineering* 384, 113959. URL: <https://www.sciencedirect.com/science/article/pii/S0045782521002966>, doi:<https://doi.org/10.1016/j.cma.2021.113959>.
- Bandai, T., Ghezzehei, T.A., 2021. Physics-informed neural networks with monotonicity constraints for richardson-richards equation: Estimation of constitutive relationships and soil water flux density from volumetric water content measurements. *Water Resources Research* 57.
- Codina, R., Vázquez, M., Zienkiewicz, O.C., 1998. A general algorithm for compressible and incompressible flows. part iii: The semi-implicit form. *International Journal for Numerical Methods in Fluids* 27, 13–32.
- Dwivedi, V., Srinivasan, B., 2020. Physics informed extreme learning machine (pielme)—a rapid method for the numerical solution of partial differential equations. *Neurocomputing* 391, 96–118. URL: <https://www.sciencedirect.com/science/article/pii/S0925231219318144>, doi:<https://doi.org/10.1016/j.neucom.2019.12.099>.
- F.R.S., G.T., 1923. Lxxv. on the decay of vortices in a viscous fluid. *The London, Edinburgh, and Dublin Philosophical Magazine and Journal of Science* 46, 671–674. URL: <https://doi.org/10.1080/14786442308634295>, doi:10.1080/14786442308634295, arXiv:<https://doi.org/10.1080/14786442308634295>.
- Jagtap, A.D., Kawaguchi, K., Karniadakis, G.E., 2020. Adaptive activation functions accelerate convergence in deep and physics-informed neural networks. *Journal of Computational Physics* 404, 109136.
- Kani, J.N., Elsheikh, A.H., 2018. Reduced order modeling of subsurface multiphase flow models using deep residual recurrent neural networks. *Transport in Porous Media*.
- Liu, D., Wang, Y., 2019. Multi-fidelity physics-constrained neural network and its application in materials modeling. *Journal of mechanical design*

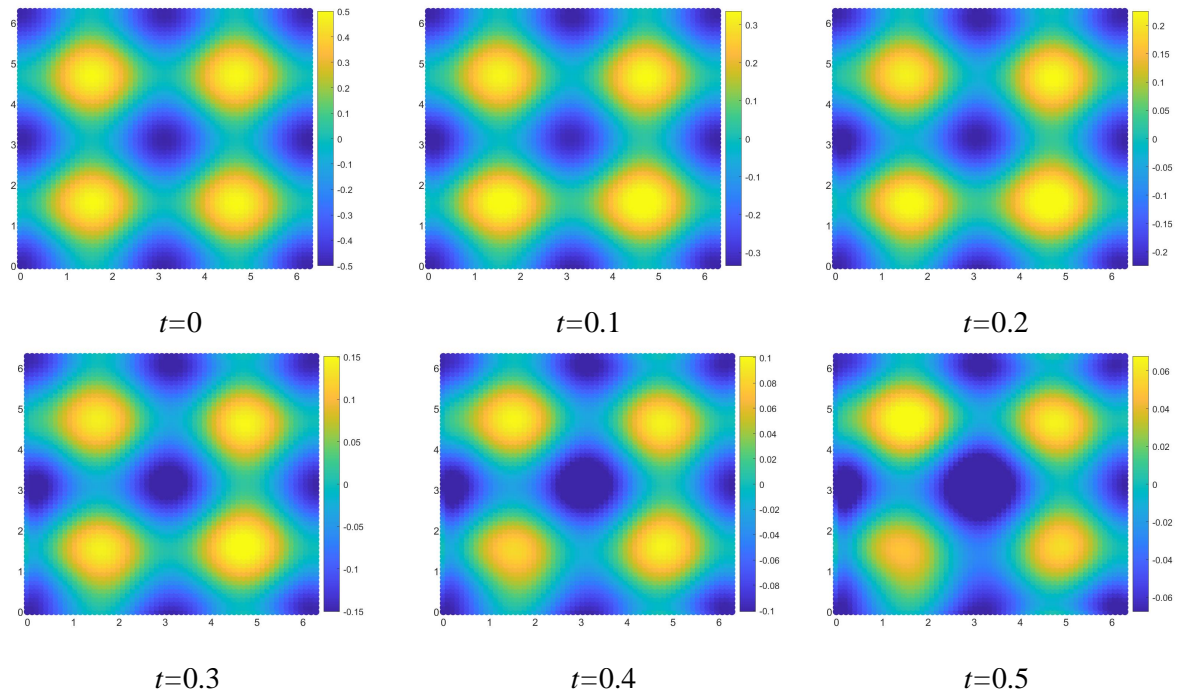


Figure 10: The spatial distribution of p . From left to right is their change with time. Boundary conditions with p . $\Delta t = 0.005$

- , 141.
- Liu, Z., Cai, W., Xu, Z.Q.J., 2020. Multi-scale deep neural network (mscalednn) for solving poisson-boltzmann equation in complex domains. *Communications in Computational Physics* 28.
- Löhner, R., Morgan, K., Zienkiewicz, O.C., 1984. The solution of non-linear hyperbolic equation systems by the finite element method. *International Journal for Numerical Methods in Fluids* 4, 1043–1063.
- Long, Z., Lu, Y., Dong, B., 2019. Pde-net 2.0: Learning pdes from data with a numeric-symbolic hybrid deep network. *Journal of Computational Physics* 399, 108925.
- Long, Z., Lu, Y., Ma, X., Dong, B., 2018. Pde-net: Learning pdes from data, in: *International Conference on Machine Learning*, PMLR. pp. 3208–3216.
- Mao, Z., Jagtap, A.D., Karniadakis, G.E., 2020. Physics-informed neural networks for high-speed flows. *Computer Methods in Applied Mechanics and Engineering* 360, 112789. URL: <https://www.sciencedirect.com/science/article/pii/S0045782519306814>, doi:<https://doi.org/10.1016/j.cma.2019.112789>.
- Raissi, M., Perdikaris, P., Karniadakis, G.E., 2017a. Physics informed deep learning (part i): Data-driven solutions of nonlinear partial differential equations. *arXiv preprint arXiv:1711.10561*.
- Raissi, M., Perdikaris, P., Karniadakis, G.E., 2017b. Physics informed deep learning (part ii): Data-driven discovery of nonlinear partial differential equations. *arXiv preprint arXiv:1711.10566*.
- Raissi, M., Yazdani, A., Karniadakis, G.E., 2020. Hidden fluid mechanics: Learning velocity and pressure fields from flow visualizations. *Science* 367, 1026–1030.
- Ranade, R., Hill, C., Pathak, J., 2021. Discretizationnet: A machine-learning based solver for navier–stokes equations using finite volume discretization. *Computer Methods in Applied Mechanics and Engineering* 378, 113722. URL: <https://www.sciencedirect.com/science/article/pii/S004578252100058X>, doi:<https://doi.org/10.1016/j.cma.2021.113722>.
- Shankar, P.N., Deshpande, M., 2000. Fluid mechanics in the driven cavity. *Annual Review of Fluid Mechanics* 32.
- Snaiki, R., 2019. Knowledge-enhanced deep learning for simulation of tropical cyclone boundary-layer winds. *Journal of Wind Engineering and Industrial Aerodynamics: The Journal of the International Association for Wind Engineering* 194.
- Wang, B., Zhang, W., Cai, W., 2020. Multi-scale deep neural network (mscalednn) methods for oscillatory stokes flows in complex domains. *Communications in Computational Physics* 28, 2139–2157.
- Wang, H., Liu, Y., Wang, S., 2022. Dense velocity reconstruction from particle image velocimetry/particle tracking velocimetry using a physics-informed neural network. *Physics of fluids*, 34.
- Wang, S., Wang, H., Perdikaris, P., 2021. On the eigenvector bias of fourier feature networks: From regression to solving multi-scale pdes with physics-informed neural networks. *Computer Methods in Applied Mechanics and Engineering* 384, 113938. URL: <https://www.sciencedirect.com/science/article/pii/S0045782521002759>, doi:<https://doi.org/10.1016/j.cma.2021.113938>.
- Xu, Z., Zhang, Y., Luo, T., Xiao, Y., Ma, Z., 2020. Frequency principle: Fourier analysis sheds light on deep neural networks. *Communications in Computational Physics*.
- Xu, Z.Q.J., Zhang, Y., Xiao, Y., 2019. Training behavior of deep neural network in frequency domain, in: Gedeon, T., Wong, K.W., Lee, M. (Eds.), *Neural Information Processing*, Springer International Publishing, Cham. pp. 264–274.
- Yang, L., Meng, X., Karniadakis, G.E., 2021. B-pinns: Bayesian physics-informed neural networks for forward and inverse pde problems with noisy data. *Journal of Computational Physics* 425, 109913. URL: <https://www.sciencedirect.com/science/article/pii/S0021999120306872>, doi:<https://doi.org/10.1016/j.jcp.2020.109913>.
- Zienkiewicz, O., Taylor, R., Nithiarasu, P. (Eds.), 2014. *The Characteristic-Based Split (CBS) Algorithm*. seventh edition ed.. Butterworth-Heinemann, Oxford. pp. 87–118. URL: <https://www.sciencedirect.com/science/article/pii/B9781856176354000340>, doi:<https://doi.org/10.1016/C2009-0-26328-8>.